Phospholipase C-related but catalytically inactive proteins regulate ovarian follicle development

Received for publication, September 22, 2016, and in revised form, March 29, 2017 Published, Papers in Press, March 30, 2017, DOI 10.1074/jbc.M116.759928

Miho Matsuda[‡1] **and Masato Hirata**[‡§]

From the [‡]*Laboratory of Molecular and Cellular Biochemistry, Faculty of Dental Science, Kyushu University, Fukuoka 812-8582, Japan and the* [§]*Fukuoka Dental College, Fukuoka 814-0193, Japan*

Edited by Xiao-Fan Wang

Phospholipase C-related but catalytically inactive proteins PRIP-1 and -2 are inositol-1,4,5-trisphosphate binding proteins that are encoded by independent genes. Ablation of the *Prip* genes in mice impairs female fertility, which is manifested by fewer pregnancies, a decreased number of pups, and the decreased and increased secretion of gonadal steroids and gonadotropins, respectively. We investigated the involvement of the PRIPs in fertility, focusing on the ovaries of *Prip-1* and *-2* double-knock-out (DKO) mice. Multiple cystic follicles were observed in DKO ovaries, and a superovulation assay showed a markedly decreased number of ovulated oocytes. Cumulus-oocyte complexes showed normal expansion, and artificial gonadotropin stimulation regulated the ovulation-related genes in a normal fashion, suggesting that the ovulation itself was probably normal. A histological analysis showed atresia in fewer follicles of the DKO ovaries, particularly in the secondary follicle stages. The expression of luteinizing hormone receptor (LHR) was aberrantly higher in developing follicles, and the phosphorylation of extracellular signal-regulated protein kinase, a downstream target of LH-LHR signaling, was higher in DKO granulosa cells. This suggests that the up-regulation of LH-LHR signaling is the cause of impaired follicle development. The serum estradiol level was lower, but estradiol production was unchanged in the DKO ovaries. These results suggest that PRIPs are positively involved in the development of follicles via their regulation of LH-LHR signaling and estradiol secretion. Female DKO mice had higher serum levels of insulin, testosterone, and uncarboxylated osteocalcin, which, together with reduced fertility, are reminiscent of polycystic ovary syndrome in humans.

The reproductive system is one of the fundamental systems regulated by hormones in living organisms. Follicle development, ovulation, and fertilization are the key events in mammalian female reproduction. The female system is regulated by the hypothalamic-pituitary-gonadal (HPG)[2] axis (1) and is subjected to complex hormonal regulation by gonadotropin-releasing hormone (GnRH), follicle-stimulating hormone (FSH), luteinizing hormone (LH), estrogen, and progesterone. The female reproductive system is more vulnerable to dysregulation of the HPG axis than the male system, and related aberrant conditions include irregular estrous cycle, precocious puberty, and polycystic ovary syndrome (PCOS) (2, 3). The etiology of these conditions is still only partially understood, and the molecular and cellular mechanisms are largely unknown.

Phospholipase C-related but catalytically inactive proteins PRIP-1 and -2 were first identified as D-*myo*-inositol 1,4,5-trisphosphate ($Ins(1,4,5)P_3$) binding proteins (4, 5). They were named because they lacked catalytic activity, despite having a domain organization that is similar to phospholipase C-δ1, which includes a pleckstrin homology (PH) domain, EF-hand motifs, catalytic X and Y, and C2 domains (6, 7). Several interacting partners have been identified for PRIPs, including γ-aminobutyric acid type A ($GABA_A$) receptor-associated protein (8), the β subunit of the $GABA_A$ receptor (9), the catalytic subunits of protein phosphatase 1α and 2A (9, 10), the phosphorylated form of Akt (11), and SNARE proteins (12, 13), in addition to $Ins(1,4,5)P_3$ and phosphatidylinositol 4,5-bisphosphate (14, 15). The discovery of these binding partners led to the identification of the involvement of PRIPs in $Ins(1,4,5)P_3/Ca^{2+}$ signaling (14, 16), $GABA_A$ receptor signaling (17–19), protein dephosphorylation (20, 21), and exocytosis (12, 13). It was also found that PRIPs are involved in the regulation of bone formation (22, 23) and bone resorption (24).

Interestingly, *Prip-1* and *-2* double-knock-out (DKO) male and female pairs exhibited decreased fertility and a smaller litter size, indicating dysfunction of the reproductive system. Cross-mating experiments with wild-type (WT) and DKO mice revealed that the defect resides in females (25). We then investigated the HPG axis in DKO females and found higher serum levels of LH and FSH, an unclear LH surge, and lower serum levels of gonadal steroid hormones (25). The isolated anterior lobes of the pituitary glands from DKO females secreted more gonadotropins in response to a gonadotropin-releasing-hormone-mimicking peptide in comparison to WT females, sug-

This work was supported by Grant-in-Aid for Scientific Research, KAKENHI Grants: 24229009 (to M.H.) and 24592804 (to M.M.) from the Japan Society for the Promotion of Science. The authors declare that they have no conflicts of interest with the contents of this article.

[1] To whom correspondence should be addressed: 3-1-1 Maidashi, Higashi-ku, Fukuoka 812-8582, Japan. Tel.: 81-92-642-6321, Fax: 81-92-642-6322; E-mail: natural@dent.kyushu-u.ac.jp.

[2] The abbreviations used are: HPG, hypothalamic-pituitary-gonadal axis; CL, corpus luteum; COC, cumulus-oocyte complex; Bt_2cAMP, dibutyryl cyclic AMP; DKO, *Prip-1* and *-2* double-knockout; E2, 17β-estradiol; ERK, extracellular signal-regulated kinase; GEO, Gene Expression Omnibus; H&E, hematoxylin and eosin; hCG, human chorionic gonadotropin; LH, luteinizing hormone; LHR, luteinizing hormone receptor; MAPK, mitogen-activated protein kinase; OC, osteocalcin; PRIP (*Prip*), phospholipase C-related but catalytically inactive protein (gene); PGE_2, prostaglandin E_2; PCOS, polycystic ovary syndrome; PMSG, pregnant mare serum gonadotropin; qPCR, quantitative real-time polymerase chain reaction; PH, pleckstrin homology; $Ins(1,4,5)P_3$, D-*myo*-inositol 1,4,5-trisphosphate.

gesting that the higher secretion of gonadotropin that was observed does not occur through a feedback loop in the HPG axis (25). These results and our previous studies suggest that PRIPs are negatively involved in exocytosis in the pituitary gland, which leads to the secretion of peptide hormones (12, 13, 25).

In the present study, we histochemically and biochemically investigated the DKO ovaries and found impaired follicle development, which appeared to occur through the up-regulation of LH-LH receptor (LHR) signaling, and the impaired secretion of estradiol from granulosa cells. The phenotype partly resembles PCOS, which is one of the most common endocrinopathies affecting women of reproductive age worldwide (3, 26, 27).

Results

A decrease in the number of ovulated oocytes in DKO mice

Because a higher serum gonadotropin level is likely to affect the ovarian function, we first examined the DKO ovaries' response to gonadotropins. Female mice were subjected to a standard superovulation assay. After injecting the mice with pregnant mare serum gonadotropin (PMSG) and human chorionic gonadotropin (hCG), the ovulated oocytes were collected from the oviducts and counted. In 3-week-old DKO mice, the total number of ovulated oocytes decreased to about one-fifth of that in age-matched WT females (Fig. 1*A*). DKO mice at 12 weeks also showed fewer ovulated oocytes. A histological analysis showed that, whereas each WT ovary showed several corpora lutea (CLs), the DKO ovaries showed few CLs and an increased number of developing follicles, such as secondary or preantral follicles (Fig. 1*B*).

When the mice were treated with PMSG only, the DKO ovaries were similar to the WT ovaries in size and weight. However, the DKO ovaries appeared cystic, and histological analyses confirmed the presence of follicular cysts with hemorrhagic and/or atretic appearances (Fig. 2, *A* and *B*). Similar appearance was also observed in DKO ovaries untreated with PMSG (Fig. 2, *A* and *B*). The DKO ovaries in mice treated with PMSG contained about four times more cystic follicles than the WT ovaries did (Fig. 2*B*). WT ovaries in mice untreated with PMSG showed few cystic follicles, probably because of the condition with various stages of estrous cycle, but several cystic follicles were clearly observed in DKO ovaries (Fig. 2*B*). An abnormal status of luteinizing and hemorrhagic follicles, encompassing trapped oocytes, was also observed in the DKO ovaries, but not in the WT ovaries (Fig. 2*C*). These results indicate that the PRIP deficiency impairs follicle development and possibly ovulation itself.

The effect of PRIP deficiency on the ovulation process

To examine the effect of PRIP deficiency on the ovulation process, Cumulus-oocyte complex (COC) expansion was examined *in vivo* in DKO mice. The COC is an important complex in which intercellular communication between the cumulus cells and between the cumulus cells and the oocytes occurs *via* an extensive network of gap junctions. The COC expansion is required for ovulation after the LH surge (28, 29). Expanded COCs, which had a normal appearance, were obtained from the oviducts of the DKO mice after treatment with PMSG and hCG

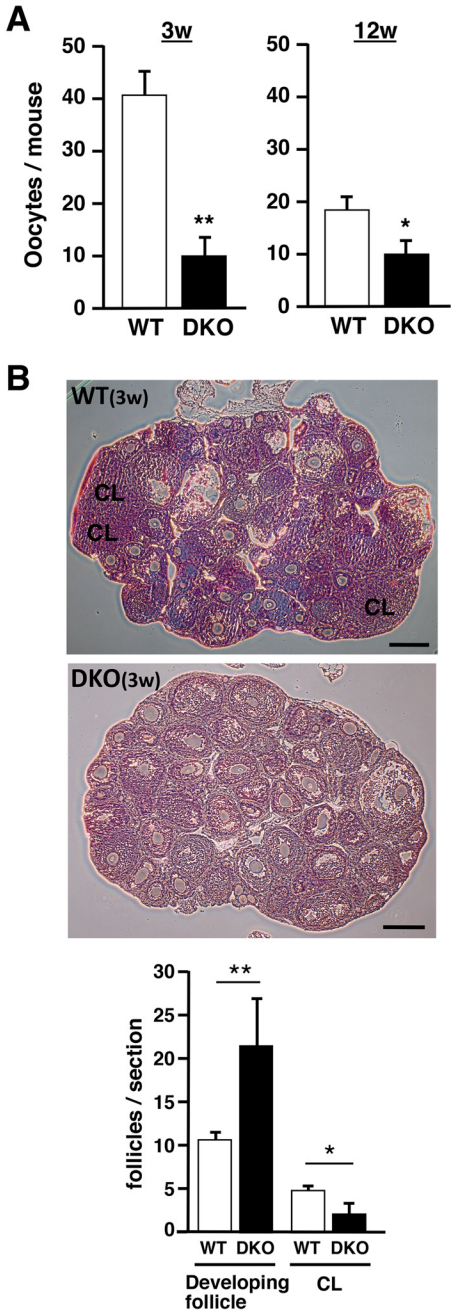

Figure 1. The superovulation assay. *A*, the numbers of ovulated oocytes per mouse. The data are presented as the mean ± S.D. The female mice of indicated ages ($n = 5$ for each genotype) were treated with PMSG and hCG and the ovulated oocytes were collected and counted. *, $p < 0.05$, **, $p < 0.01$. *B*, histological analysis of the ovaries from 3-week-old mice after superovulation. *Upper panels* show H&E-stained histological images of the ovaries. *Scale bar*, 200 μm. The graph shows the quantification of developing follicles and CLs after superovulation. H&E-stained sections as shown in *upper panels* ($n = 5$ for each genotype; at least four sections of each ovary) were used. Developing follicles contain secondary, preantral, and antral follicles. The criteria for evaluation of those follicles are described under "Experimental Procedures."

(Fig. 3*A*). This indicates that the whole ovulation process (*i.e.* COC expansion, follicle rupture, COC extrusion, and transfer to the oviduct) occurred normally in DKO mice.

COC expansion was also examined *in vitro* using COCs isolated from the ovaries of PMSG-treated mice. The expansion was similarly observed in COCs from DKO and WT at 18 h after induction by EGF (Fig. 3, *B* and *C*). Prostaglandin E_2 (PGE_2) and

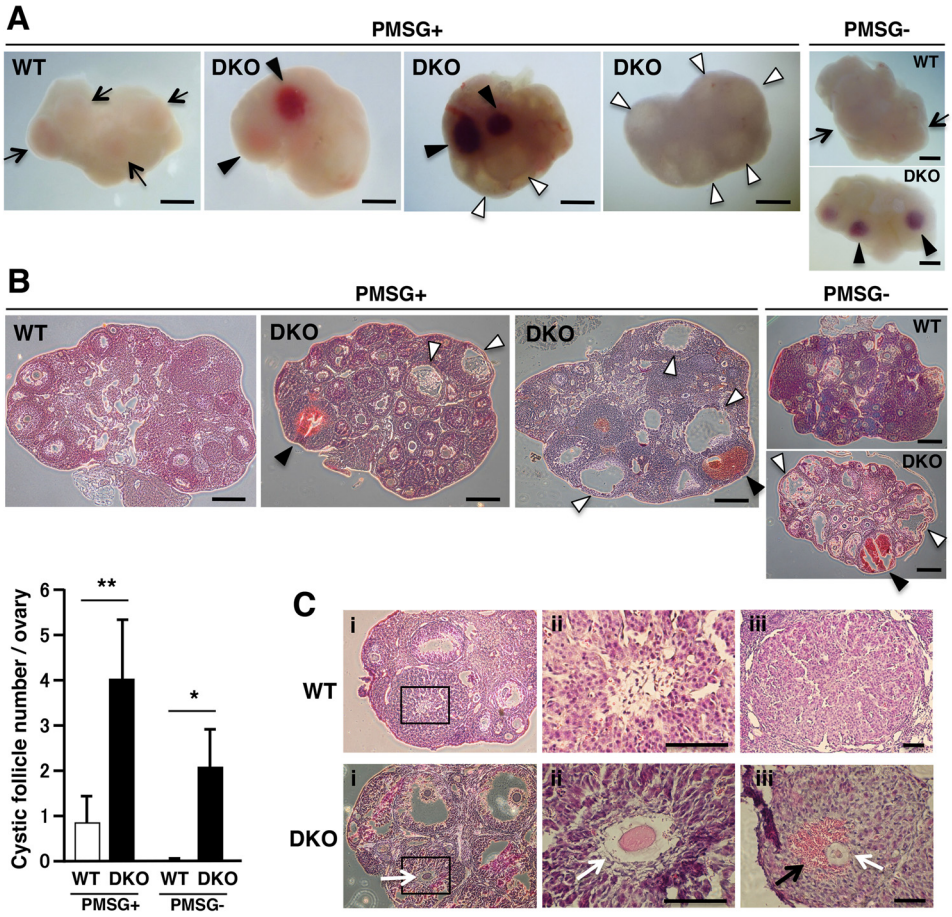

Figure 2. The histological analysis of the preovulatory ovaries. *A*, gross images under a binocular microscope. The ovaries of mice (age 5–6 weeks) were dissected at 48 h after PMSG treatment (PMSG+) and also dissected without the treatment (PMSG−). Arrows show the protrusion of preovulatory follicles. In both *A* and *B*, the *black* and *white arrowheads* show hemorrhagic cysts and arrested follicular cysts, respectively. *Scale bars*, 500 μm. *B*, H&E-stained histological images of the above ovaries. *Scale bars*, 300 μm. The graph shows the average number of cystic follicles per ovary ($n = 4$ for each genotype). A cystic follicle was defined as a cyst lined by one to several layers of attenuated granulosa cells surrounded by unclear theca cell layer, and with a faded oocyte. The data are expressed as the mean ± S.D. *, $p < 0.05$; **, $p < 0.01$. *C*, histological images of luteinizing follicles with trapped oocytes indicated by *white arrows* in DKO ovaries. *Panel ii* shows a magnified image of the *rectangle* in *panel i*. *Panel iii* in DKO shows a trapped oocyte surrounded by red blood cells (*black arrow*). *Scale bars*, 50 μm.

dibutyryl cyclic AMP (Bt_2cAMP), a membrane-permeable cAMP analog, are also known to trigger this process by initiating the synthesis and/or secretion of hyaluronan, an essential constituent of the expanded cumulus matrix. PGE_2 and Bt_2cAMP elicited expansion similarly in DKO and WT COCs (Fig. 3, *B* and *C*).

The expression of the genes related to the ovulation process, including the COC expansion step, was examined in a microarray analysis using RNA purified from the ovaries of mice treated with PMSG alone or with PMSG and hCG. The expression of multiple genes that are important for ovulation was increased to a similar extent in DKO and WT ovaries after hCG stimulation (data not shown). To confirm the microarray results, a quantitative real-time polymerase chain reaction (qPCR) was performed with the same RNA preparations for a selected set of ovulation-related genes. It was found that the expression levels of *Ereg* (epiregulin, a member of the EGF-like family and a ligand of the EGF receptor), *Tnfaip6* (tumor necrosis factor-α-induced protein 6, a hyaluronan-binding molecule), *Has2* (hyaluronan synthase-2), and *Ptgs2* (prostaglandin-endoperoxide synthase 2) in DKO ovaries were higher than those in WT ovaries after PMSG treatment (Fig. 4*A*). However, hCG stimulation increased the expression of *Ereg*, *Tnfaip6*, *Has2*, *Ptgs2*, and *Ptx3* (pentraxin 3, a protein involved in the stability of the cumulus cell matrix) in both WT and DKO ovaries to similar levels. In contrast, hCG stimulation led to a slight decrease in the expression of *Ptger2* (PGE_2 receptor), but again the levels in the WT and DKO ovaries were similar. Thus, both the dynamics and the final levels of expression of the ovulation-related genes were largely unaffected in the DKO ovaries after hCG stimulation. Similar results were obtained from the gene expression analysis using RNA purified from COCs isolated from the ovaries of mice treated with PMSG alone or along with hCG, but the expression of *Ereg* and *Tnfaip6* was slightly decreased in DKO mice with PMSG alone (Fig. 4*B*). In mice without any treatment, those gene expressions were similar between WT and DKO COCs (Fig. 4*C*).

The effect of PRIP deficiency on follicle development

The above-described results suggest that the decreased number of ovulated oocytes in DKO female mice was attributable to defective follicle development rather than ovulation. We then examined the number of follicles at each developmental stage in the ovaries at 4–5 weeks and found that there were increased

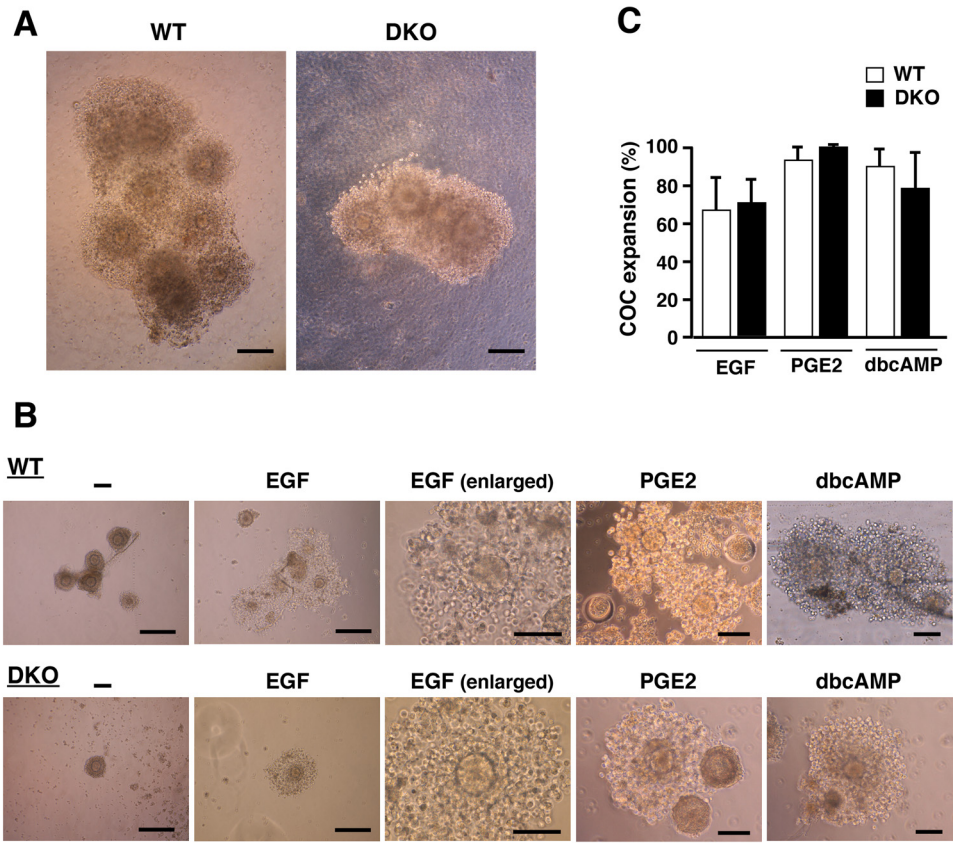

Figure 3. The COC expansion analysis. *A*, typical images of expanded COCs isolated from the oviducts after superovulation. *Scale bars*, 100 μm. *B*, images of COCs induced to expand *in vitro*. COCs isolated from the preovulatory follicles 46 h after treatment with PMSG were cultured with EGF (10 ng/ml), PGE_2 (1.4 μM), or Bt_2cAMP (2 mM) for 18 h and observed. *Scale bars*, no stimulation or EGF, 100 μm; EGF (enlarged), PGE_2, and Bt_2cAMP, 30 μm. *C*, the quantification of COC expansion *in vitro*. The graph shows a ratio of the number of expanded COCs to that of total COCs in the treatment with EGF, PGE2, and Bt_2cAMP (*dbcAMP*), respectively. Two to five COCs were used for the expansion experiments per a treatment and five mice of each genotype were used. The data are expressed as the mean ± S.D.

numbers of less-developed follicles, such as secondary and preantral follicles, and decreased numbers of preovulatory follicles, and possibly antral follicles and CLs, in DKO ovaries in comparison with WT ovaries after PMSG treatment (Fig. 5*A*). To investigate the cause of these observations and the presence of follicular cysts with an atretic appearance (Fig. 2), apoptotic follicles were observed using a TUNEL assay (Fig. 5*B*). Follicle atresia, which affects all stages of follicle development, is required for the production of mature follicles and depends on the apoptosis of granulosa cells. The total number of TUNEL-positive follicles was smaller in DKO ovaries, especially in the secondary follicle stage (Fig. 5, *B* and *C*). These differences between WT and DKO ovaries were similarly observed in mice untreated with PMSG (Fig. 5*D*). These results suggest that the impairment of follicle development occurs as early as the secondary follicle stage in DKO ovaries.

The expression and the downstream signaling of LHR in DKO ovaries

The granulosa cells in preovulatory follicles are fully differentiated and express high levels of LHR, whereas those in developing follicles express high levels of the FSH receptor and low levels of LHR. To examine the LHR expression in DKO follicles, ovarian sections from PMSG-treated mice were immunohistochemically examined. In the WT ovaries, granulosa cells in the developing follicles of the secondary and preantral stages expressed very little LHR, whereas the theca cells in the same follicles and CLs clearly expressed LHR (Fig. 6*A*). The expression of LHR was observed in the granulosa cells of the developing follicles in the DKO ovaries (Fig. 6*A*). A quantitative analysis of the immunofluorescence intensity indicated that LHR was more highly expressed in the granulosa cells of DKO follicles (Fig. 6*B*).

Both PRIP-1 and -2 were present in the granulosa cells isolated from the WT ovaries of PMSG-treated mice (Fig. 7*A*), suggesting that these proteins may regulate the expression or downstream signaling of LHR. The expression of PRIP-1 and -2 was confirmed in the cells isolated from WT ovaries of mice without PMSG treatment (data not shown). We then confirmed the higher expression of LHR in DKO granulosa cells, but no difference was seen with FSHR (Fig. 7*B*). These expression patterns of the receptors in WT and DKO cells were similarly observed in the cells isolated from younger mice without PMSG treatment (Fig. 7*E*). Upon exposure to hCG, the DKO cells showed a greater and longer phosphorylation of ERK, a downstream target of the LH-LHR signaling. The basal level of phosphorylation also appeared to be higher in DKO cells, although this difference was not statistically significant (Fig. 7*C*). The phosphorylation of ERK by hCG was blocked by

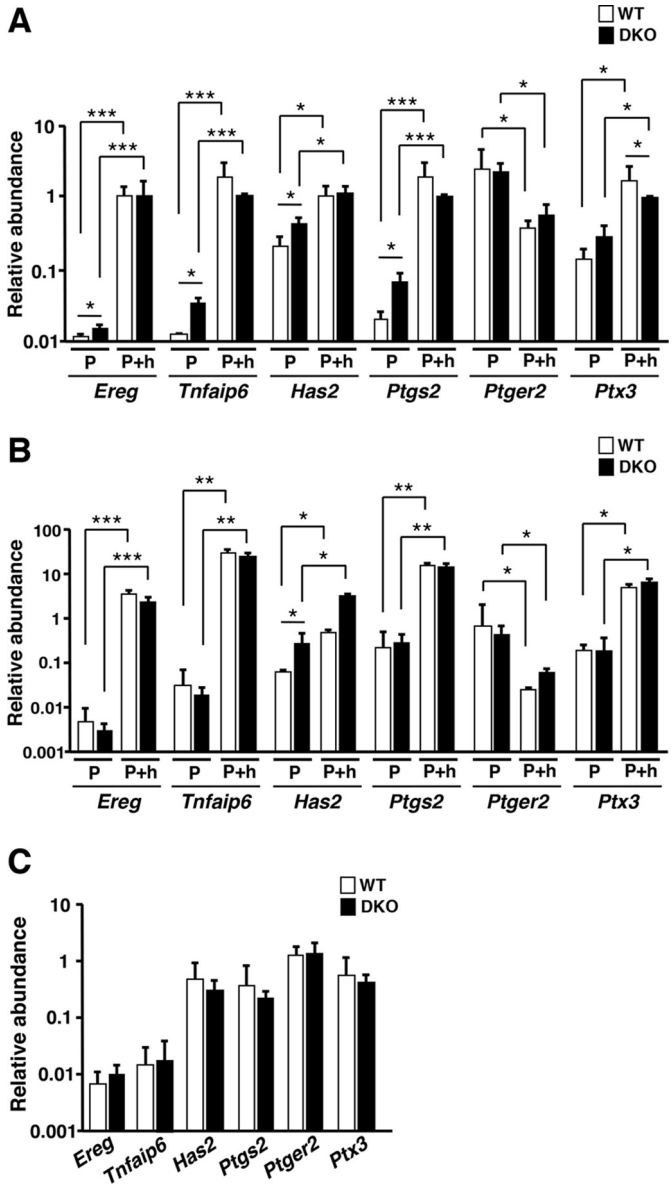

Figure 4. The gene expression analysis. *A*, female mice (age 4 weeks, $n = 4$ for each genotype) were sacrificed 48 h after PMSG for injection, or 4 h after hCG injection in addition to the PMSG treatment. RNA was purified from the ovaries and used for a quantitative PCR. *B* and *C*, same analysis as *A* was performed using COC. RNA was purified from COCs isolated from the ovaries of mice treated with PMSG alone or along with hCG respectively (*B*), and isolated from the ovaries of mice without any treatment (*C*). The data are expressed as the mean ± S.D. The relative gene expression was determined by normalization against *Gapdh*. *Ereg*, epiregulin; *Tnfaip6*, tumor necrosis factor-α-induced protein 6; *Has2*, hyaluronan synthase-2; *Ptgs2*, prostaglandin-endoperoxide synthase 2; *Ptger2*, PGE_2 receptor; *Ptx3*, pentraxin 3. *, $p < 0.05$; **, $p < 0.01$; ***, $p < 0.001$.

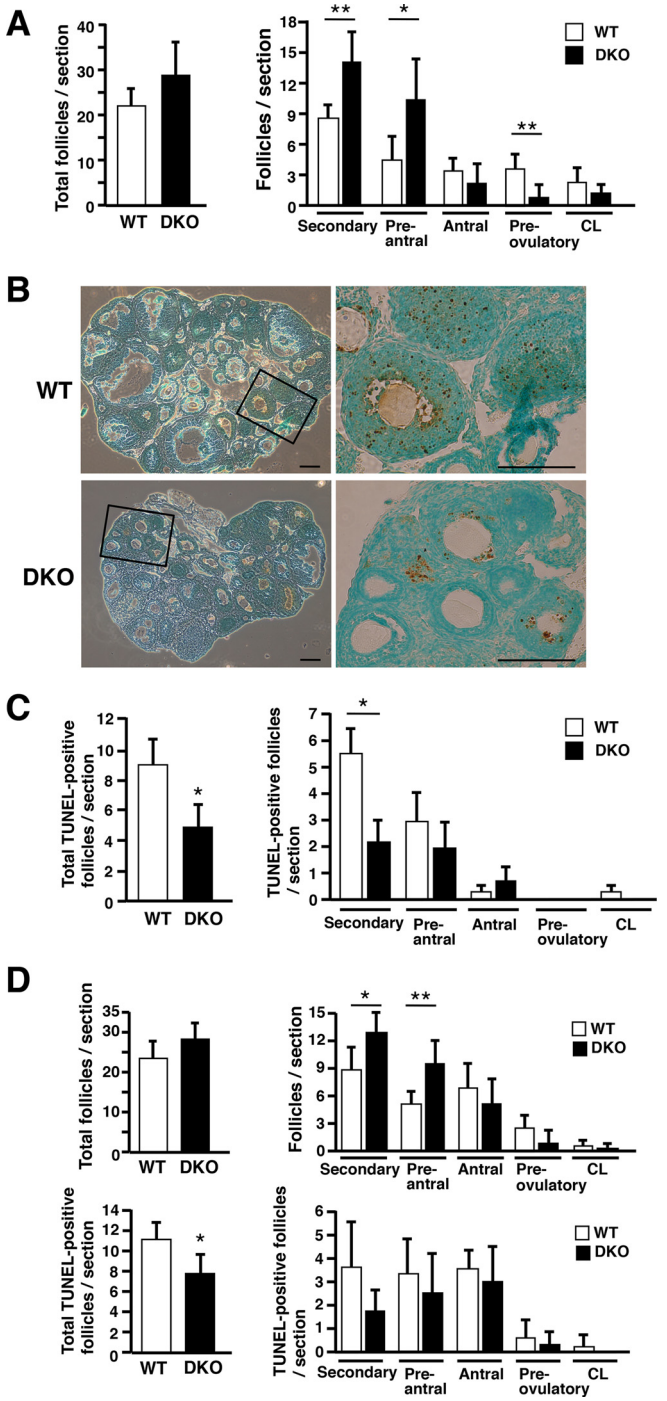

Figure 5. The developmental stages of the follicles. *A*, the total follicle numbers (*left panel*) and the numbers of follicles at various stages (*right panel*) determined in ovary sections. The ovaries of the mice (age, 4–5 weeks; $n = 5$ for each genotype) were dissected at 48 h after PMSG treatment. At least four H&E-stained sections of each ovary were used to count follicles in each developing stage, according to the histological criteria of follicle stages described under "Experimental Procedures." *B*, the TUNEL assay for the detection of atretic follicles. The follicles containing TUNEL-positive cells (colored *brown*) indicate the atretic ones. Sections were counterstained with methyl green. The areas outlined with *rectangles* are enlarged in the *right-hand panels*. *Scale bars*, 200 μm. *C*, the total numbers of TUNEL-positive follicles (*left panel*) and the numbers of TUNEL-positive follicles at various stages (*right panel*). TUNEL-positive follicles in various stages were also counted using at least four sections per ovary as well as the counting in H&E sections. *D*, the analyses described above were also performed using the ovaries of the mice (age, 6 weeks; $n = 5$ for each genotype) without PMSG treatment. The data were obtained from at least four sections per ovary. The data are expressed as the mean ± S.D. *, $p < 0.05$; **, $p < 0.01$.

U0126, an inhibitor of MAPK kinases, in both genotype cells (Fig. 7*C*). Greater ERK phosphorylation was observed in the ovaries of DKO mice that were only treated with PMSG; however, no significant difference was observed between the two genotypes after stimulation with hCG (Fig. 7*D*). The elevated level of ERK phosphorylation was also observed in DKO granulosa cells and whole ovaries isolated from younger mice without any treatment (Fig. 7*E*). These results suggest that the excessive downstream signaling activity of LHR in DKO mice

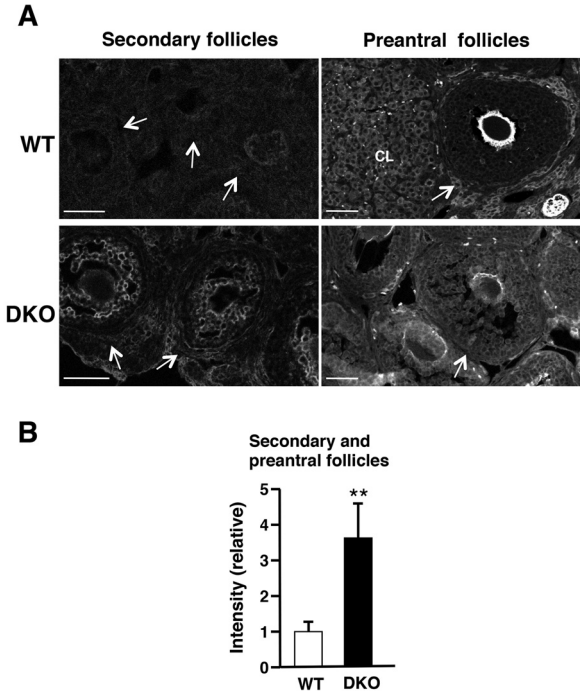

Figure 6. The expression of LHR in the follicles. *A*, typical images of immunohistochemical staining of LHR. Cryosections of the ovaries were immunostained with anti-LHR antibodies. *Arrows* show the secondary and preantral follicles. The zona pellucida shows nonspecific staining. *B*, the quantification of LHR in the secondary and preantral follicles. The relative immunostaining intensities are expressed as the mean ± S.D. of 4–5 mice each. *, $p < 0.05$; **, $p < 0.01$. *Scale bars*, 50 μm.

might have been caused, at least in part, by the higher levels of LH and LHR.

Hormone levels in DKO mice

17β-estradiol (E2) is one of the most important hormones in follicle development, and androgen is also important for follicle growth. Using serum samples collected at various stages of the estrous cycle, we previously reported that the serum E2 level tends to be lower in DKO mice (25). In the present study, we measured the levels of E2 and testosterone in serum samples from mice that were primed with PMSG. The serum E2 level was markedly lower in DKO samples taken at 24 and 48 h after the injection of PMSG (Fig. 8*A*); however, the serum testosterone level was higher in DKO mice (Fig. 8*B*). We also measured the E2 content in DKO ovaries; it was higher in DKO ovaries, indicating that the production of E2 in DKO ovaries is not impaired (Fig. 8*A*).

In the course of the above studies, we realized that the results obtained from DKO mice, including increased numbers of developing follicles and follicular cysts, the marked reduction in the number of ovulated oocytes, the decreased serum E2 level, and the increased serum testosterone and LH levels (25), are reminiscent of PCOS. Because hyperinsulinemia is another major pathological feature of PCOS, we measured the serum insulin level of DKO mice. Both fasted and fed female DKO mice exhibited higher serum insulin levels than female WT mice (Fig. 8*C*). The serum level of osteocalcin (OC), a bone-derived hormone that has been recently implicated in the pathogenesis of PCOS, was also measured. Female DKO mice exhibited a higher level of uncarboxylated OC (Fig. 8*D*), similarly to lean women with PCOS (30). Intriguingly, the mining of the Gene Expression Omnibus (GEO) data (ID: GDS3841) showed decreased mRNA levels of both *PRIP-1* and *-2* in the cumulus cells from lean women with PCOS (Fig. 8*E*).

Discussion

The present study provides evidence that PRIPs are involved in the regulation of follicle development, which explains the reduced female fertility (25) and the marked decrease in the number of ovulated oocytes (Fig. 1) in *Prip-1* and *-2* DKO mice. We also found, in addition to the higher serum level of LH (25), the higher expression of LHR in DKO granulosa cells (Figs. 6 and 7), which was not so evident in the whole ovaries in a previous study (25). In contrast, the expression level of FSHR in DKO cells was not significantly different from that in WT cells. Although granulosa cells normally start to express LHR at about the antral follicle stage (31, 32), those in DKO mice express LHR as early as the secondary follicle stage. Thus, not only the expression level, but also the temporal regulation of LHR is affected in DKO mice. This appears to lead to the increased phosphorylation of ERK1/2, a downstream factor of the LH-LHR signaling pathway, in DKO granulosa cells before and after hCG stimulation (Fig. 7*C*). Increased ERK1/2 phosphorylation in the basal state also occurs in DKO mice (Fig. 7*D*). The elevated LH-LHR signaling in granulosa cells may impair follicle development, which could result in an increased number of developing follicles, a decreased number of TUNEL-positive follicles, premature luteinization, and an increased number of cysts with or without hemorrhage (Figs. 2 and 5).

A recent study suggested that chronic LH stimulation impairs the FSH-induced follicle development during the preantral-antral transition in rat follicle culture (33). DKO ovaries showed similar phenotypes such as the increased number of secondary and preantral follicles (Fig. 5). The elevated LH-LHR signaling in granulosa cells at an earlier stage may also lead to the premature terminal differentiation of follicles in DKO mice, resulting in the down-regulation of follicle atresia, premature luteinization, and an increased number of aberrant cysts. A recent study showed that human LHR appears in the granulosa cells of early antral follicles and increases with follicle development (34). A greater than normal increase in human LHR expression leads to oocyte malfunction, which reduces the capacity of fertilization (32, 35). Furthermore, the overexpression of human LHR mRNA has been observed in granulosa cells from polycystic ovary patients (36). The level and stage of LHR expression might be essential for follicle development.

Consistent with the elevated LH-LHR signaling in the basal state, the serum E2 level is lower in DKO mice (Fig. 8). This may be another cause of impaired follicle development and a reduction in the number of ovulated oocytes. Because DKO mice showed a higher serum testosterone level (Fig. 8), the functional level of sex hormone-binding globulin (SHBG), a transporter of and reservoir for E2 and testosterone (37), is probably unaffected. Furthermore, the production of E2 in the granulosa cells appears to be unaffected (Fig. 8). We therefore hypothesize that

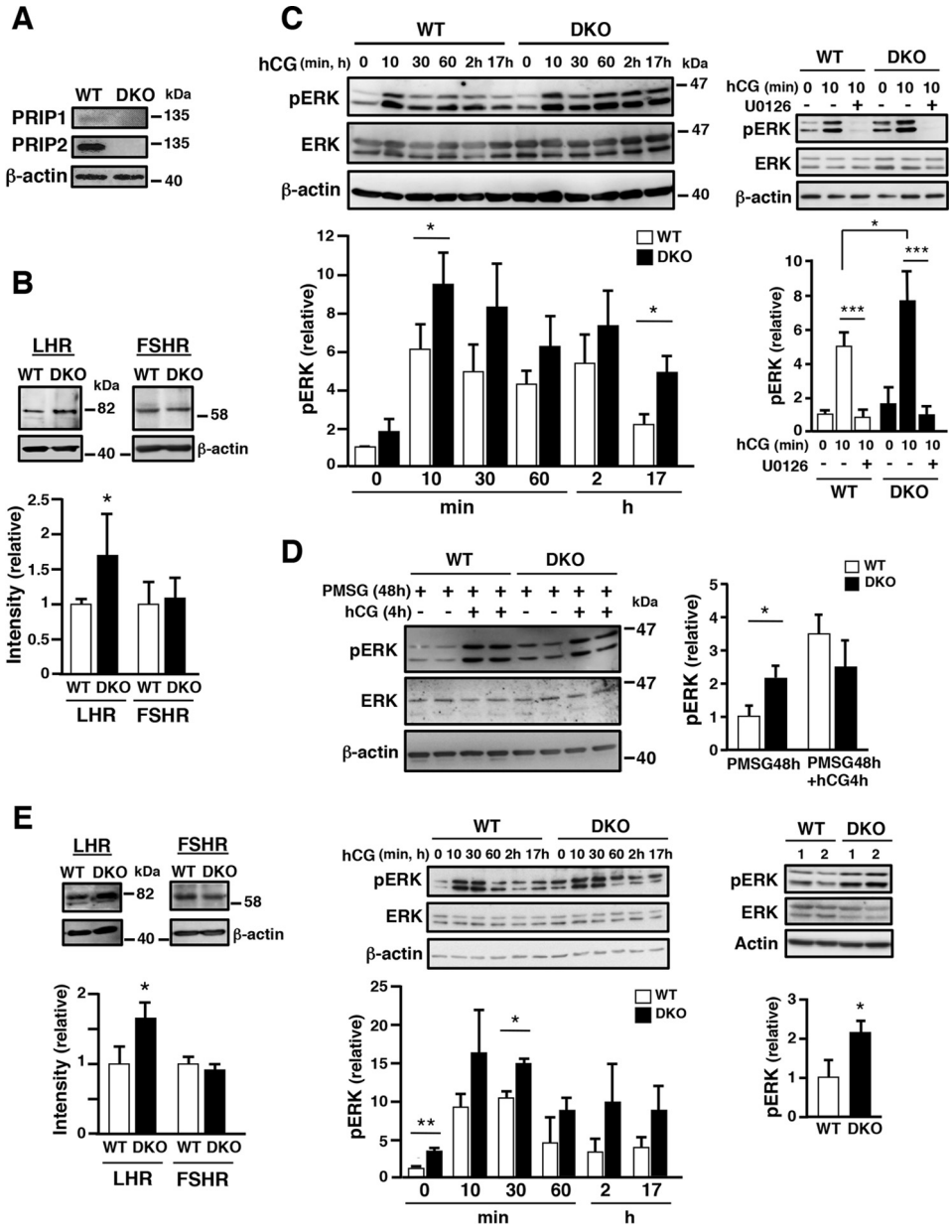

Figure 7. The expression of PRIPs, LHR and FSHR, and the phosphorylation of ERK1/2. *A*, immunoblotting of PRIP-1 and -2 in isolated granulosa cells. The cells were prepared from the ovaries of mice (age 3–4 weeks) at 47 h after PMSG treatment. *B*, immunoblotting analysis of LHR and FSHR in granulosa cells. Four mice of each genotype were used for quantification. *C*, the time course of ERK1/2 phosphorylation in granulosa cells after hCG stimulation. *Left panel* shows the time course of ERK1/2 phosphorylation and *right panel* shows the inhibition by MAPK kinase inhibitor (U0126, 5 μM). The level of phosphorylation was normalized by the total amount of ERK and is shown in the graphs, respectively. Immunoblotting was performed using anti-phospho-ERK, anti-ERK, and anti-β-actin antibodies. Four mice of each genotype were used for quantification. *D*, ERK1/2 phosphorylation in the whole ovaries. Lysates were prepared from the ovaries of mice ($n = 5$) at 48 h after PMSG treatment or at 4 h after additional hCG treatment and immunoblotting was performed. The level of phosphorylation was normalized by the total amount of ERK and is shown in the graph. *E*, immunoblotting analyses of LHR, FSHR and the time course of ERK1/2 phosphorylation in granulosa cells, and ERK1/2 phosphorylation in the whole ovaries. These analyses were performed as described above, using whole ovaries or granulosa cells isolated from the ovaries of mice (age 2–3 weeks) without any treatment. *Lanes 1* and *2* in the *right panel* show the samples derived from individual mouse. The results are shown as the mean ± S.D. *, $p < 0.05$; ***, $p < 0.001$.

the secretion process is impaired. It is thought that E2 diffuses into the extracellular space through the plasma membrane, but the precise secretory mechanism is unknown. PRIPs may be positively involved in the regulation of E2 secretion from ovary. Decreased serum level of E2 would induce gonadotropins secretion by a feedback loop to lead to increased LHR expression and/or the downstream signaling. In addition, as described in the Introduction, PRIP deficiency itself promoted the secretion of LH from the pituitary gland (25).

Healthy aging women start to exhibit the hypersecretion of gonadotropins, including LH, around menopause, which causes the malfunction of the reproductive cycle and failure in follicle development. In women of reproductive age, a high LH level and the subsequent up-regulation of LH-LHR signaling triggers premature menopause, PCOS, and other types of gynopathy. Our present and previous results (25, 38) show that DKO mice exhibit a phenotype that partly resembles PCOS, which is a common, highly heritable, and complex disorder in

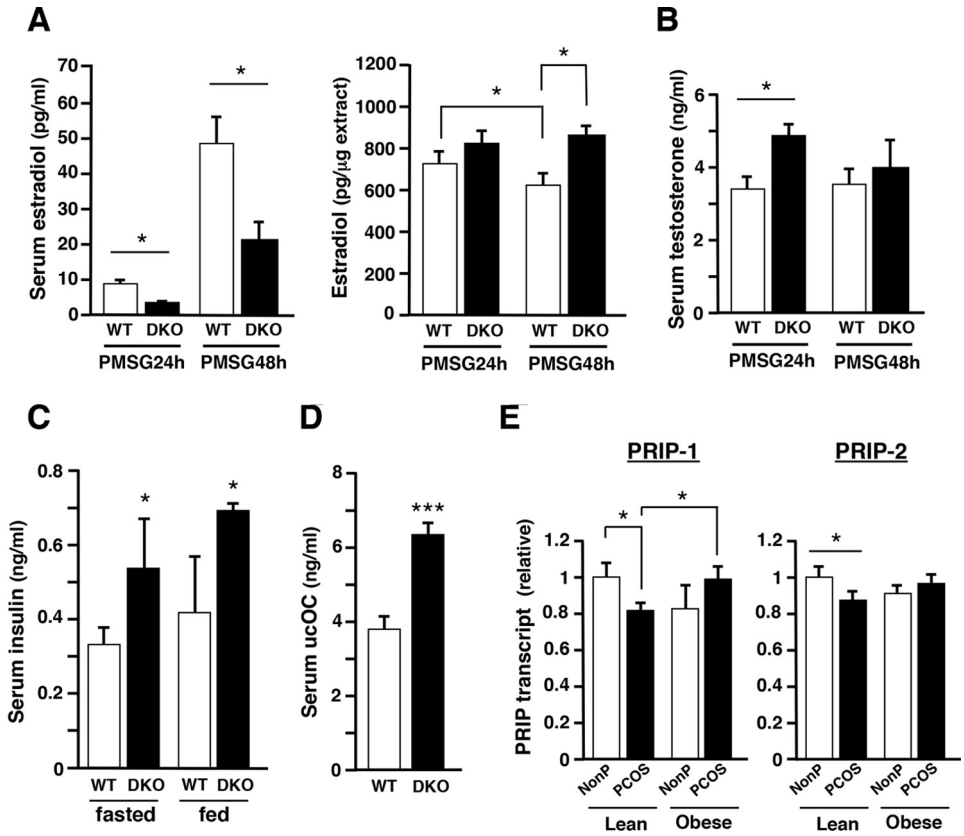

Figure 8. The measurement of hormones. *A–D*, serum samples were prepared from female mice (age 4–6 weeks, $n = 5$ for each genotype) and measured by ELISA for estradiol (*A*), testosterone (*B*), insulin (*C*), and osteocalcin (*D*). The amount of estradiol in the ovaries after blood collection was also measured and is shown in the right graph in (*A*). *ucOC*, uncarboxylated osteocalcin. *E*, the levels of *PRIP-1* and *-2* mRNAs in cumulus cells from lean and overweight-obese women with PCOS. The graphs show the results of statistical analysis of publicly available microarray data (GEO data; ID: GDS3841). The numbers of individuals studied for each of the conditions were as follows: lean non-PCOS ($n = 6$), lean PCOS ($n = 5$), obese non-PCOS ($n = 5$), and obese PCOS ($n = 7$). The value for lean women without PCOS was set at 1. nonP, non PCOS (control). The data are expressed as the mean ± S.D. *, $p < 0.05$; ***, $p < 0.001$.

women of reproductive age that is characterized by reduced fertility with various clinical and laboratory features, including chronic oligo-ovulation or anovulation, an irregular estrous cycle, increased serum LH, increased LHR, impaired follicle development, and an increased serum level of testosterone (39–42, 44). Despite its prevalence and health impact, the pathogenesis of PCOS remains unclear. The impaired follicle development in PCOS appears as follicular cysts, hemorrhagic follicles, premature luteinization (45), and increased and decreased numbers of developing and atretic follicles, respectively (46). All of these findings are observed in our DKO mice. However, although FSH and hCG treatment can induce the development of preovulatory follicles in PCOS patients, these hormones are not so effective in DKO mice. This difference suggests that DKO mice may have additional defects, which may be independent of gonadotropin signaling. PRIPs might regulate signaling pathways in addition to LH-LHR signaling which is mediated mainly *via* the Gs-protein/adenylyl cyclase/cAMP system and also could induce phospholipase C/Ins(1,4,5)P_3 *via* Gq/11 system (47) and phosphatidylinositol 3-kinase/Akt pathway directly and/or via EGF receptor pathway (48). We have reported that PRIP is involved in the regulation of phosphorylation of signaling molecules by regulating protein phosphatase 1α and 2A (9, 10), and Akt activity (11), and furthermore in the regulation of intracellular Ca^{2+} concentration *via* Ins(1,4,5)P_3 binding (14, 16). However, it is currently unknown whether the additional specific signaling pathway(s) other than LH-LHR signaling and/or molecule(s) involved in the process of follicle development are affected by PRIP deficiency.

Women with PCOS often exhibit metabolic abnormalities such as obesity, hyperinsulinemia, insulin resistance, dyslipidemia, and type 2 diabetes (49). We observe hyperinsulinemia in female DKO mice (Fig. 8), consistent with our previous study in male *Prip-1* KO mice (38). Furthermore, the pancreatic islets from DKO mice and an MIN6 beta cell line with *Prip-1* and *-2* double knockdown secrete more insulin in response to high glucose stimulation (50). PRIPs might be involved in the regulation of LH-LHR signaling through insulin secretion because insulin can stimulate the FSH-induced expression of LHR or the LHR function (51, 52). We previously showed that uncarboxylated OC increases the secretion of insulin indirectly by promoting the secretion of incretin (53). It was recently reported that the serum uncarboxylated OC level is significantly higher in lean PCOS patients (but not in obese PCOS patients) in comparison to healthy controls (30). These findings are consistent with our observations in female DKO mice (elevated uncarboxylated OC) (Fig. 8) and male DKO mice (decreased body fat mass) (54). Furthermore, our mining of the GEO database reveals the decreased mRNA levels of both *PRIP-1* and *-2* in the cumulus cells of lean women with PCOS (Fig. 8). Some DKO phenotypes such as elevated serum gonad-

otropins (25) appear to be similar to that of premature ovarian failure (POF) which is a heterogeneous disorder leading to amenorrhea and ovarian failure before the age of 40 (43). But DKO mice did not exhibit amenorrhea or depletion of follicles, main phenotype of premature ovarian failure.

In summary, this study showed that PRIPs positively regulate follicle development through LH-LHR signaling by changing the secretion of LH and the expression of LHR, and through the secretion of insulin and E2. PRIP deficiency causes a PCOS-like phenotype, including an irregular estrous cycle, decreased number of ovulated oocytes, increased numbers of follicular cysts and developing follicles. PRIP-deficient mice may provide an animal model for studying the defects in follicle development that are associated with a chronic increase in gonadotropin secretion. Because *Prips* are expressed in all of the female tissues of the HPG axis, further studies will be needed to reveal the primary site of the DKO phenotype and the precise role of PRIPs in female reproduction.

Experimental procedures

Animals

Prip-1 and *-2* DKO mice of a C57BL/6J (The Jackson Laboratory, Bar Harbor, ME) background were generated as described previously (9). The animals were maintained under a 12-h light to12-h dark cycle. The handling of mice and all of the procedures were approved by the Institutional Animal Care and Use Committee of Kyushu University and performed according to the Guidelines for Proper Conduct of Animal Experiments of the Science Council of Japan.

Superovulation assay

Female mice were intraperitoneally injected with 5 IU of PMSG (Asuka Pharmaceutical, Tokyo, Japan) and, 48 h later, with 5 IU of hCG (Asuka Pharmaceutical). The ovulated oocytes were isolated from the ampulla of the oviducts after a further 18 h.

H&E staining

The ovaries were dissected and fixed in 4% paraformaldehyde. The samples were embedded in paraffin, sectioned at 5 or 6 μm, deparaffinized, and stained with Mayer's hematoxylin and eosin (Muto Pure Chemicals, Tokyo, Japan).

The analysis of COC expansion

Female mice (age 3–4 weeks) were primed with 5 IU of PMSG. 46 h later, COCs were isolated from the ovaries by puncturing each follicular apex with a 27-gauge needle. The isolated COCs were then cultured in Dulbecco's modified Eagle's medium (DMEM)/F12 (Gibco-Invitrogen, Carlsbad, CA), supplemented with 4% fetal bovine serum (FBS) (Gibco-Invitrogen) and 100 units of penicillin-streptomycin (Gibco-Invitrogen), and stimulated with either 10 ng/ml EGF (Sigma-Aldrich), 1.4 μM PGE_2 (Cayman Chemical Company, Ann Arbor, MI), or 2 mM Bt_2cAMP (Enzo Life Sciences, Exeter, UK) at 37 °C under 5% CO_2 for 16–20 h. The extent of *in vitro* COC expansion was evaluated morphologically using an inverted microscope (IX71, Olympus, Tokyo, Japan). *In vivo* COC expansion was assessed by morphological observation of the postovulatory COCs, which were picked up from the ampulla of the oviducts of 18 h after hCG treatment.

The isolation of RNA and the analysis of gene expression

Total RNA was prepared from whole ovaries or COCs from ovaries of female mice 48 h after injection with 5 IU of PMSG, those 4 h after injection with an additional 5 IU of hCG or without any treatment. An RNeasy Mini Kit (Qiagen, Valencia, CA) was used according to the manufacturer's protocol. The total RNA was reverse transcribed to synthesize cDNA, and a qPCR was performed in a 20-μl mixture containing 2 μl of the obtained cDNA, 10 nM each primer, and KOD SYBR qPCR Mix (Toyobo, Tokyo, Japan) according to the manufacturer's instructions. The thermal cycling conditions were as follows: 35 cycles of denaturing at 95 °C for 15 s, annealing at 60 °C for 30 s, and extension at 72 °C for 30 s. The transcript level of each target gene was normalized against that of glyceraldehyde-3-phosphate dehydrogenase (*Gapdh*). A qPCR analysis was performed with Multiplate RQ (version 5, TaKaRa, Shiga, Japan) on a Thermal Cycler Dice Real Time System II (TaKaRa). The primer pairs were as follows: *Ereg* fwd: 5′-ACACTGGTCTGCGATGTGAG-3′ and rev: 5′-TCCGTAACTTGATGGCACTG-3′; *Tnfaip6* fwd: 5′-TTCCATGTCTGTGCTGCTGG-3′ and rev: 5′-AGCCTGGATCATGTTCAAGG-3′; *Has2* fwd: 5′-TGCATCGCTGCGTACCAAG-3′ and rev: 5′-ACTTCGCTGAATATGTCCATC-3′; *Ptgs2* fwd: 5′-GTACAAGCAGTGGCAAAGG-3′ and rev: 5′-CCCCAAAGATAGCATCTGG-3′; *Ptger2* fwd: 5′-GCTAATGGAGGACTGCAAG-3′ and rev: 5′-GCAGGTTCCCAGCAGGTC-3′; *Ptx3* fwd: 5′-TGGGTGGAAAGGAGAACAAG-3′ and rev: 5′-GGCCAATCTGTAGGAGTCC-3′.

The histological assessment of the follicles

The stages of follicle development were assessed using the following criteria in H&E- or TUNEL-stained ovaries. A secondary follicle was defined as a follicle composed of an oocyte surrounded by more than two layers of granulosa cells with no antrum. A preantral follicle was defined as a follicle composed of an oocyte surrounded by a multilayer of granulosa cells with a small antrum. An antral follicle was distinguished by the presence of a medium-sized antrum or more than two antra within the granulosa cell layers. A preovulatory follicle was defined as a follicle with a large antrum or with the presence of follicular fluid within the multiple granulosa cell layers. CL was defined as a large structure after ovulation, equivalent to the size of preovulatory follicles and filled with luteal cells. The number of follicles in each ovary was counted and is represented as the average per ovary section. Luteinizing follicles are those with large size, gradually filled with cells looking different from granulosa and theca cells, toward the center of follicles, and visible after ovulation to form CL. Hemorrhagic follicles containing blood clot are temporally visible in the ruptured follicles, after ovulation. If both types of follicles are visible before ovulation, fully filled with hemorrhage or contain oocytes, those follicles are judged in abnormal states.

TUNEL staining

Mouse ovaries were fixed in 4% paraformaldehyde for 4 h, embedded in paraffin, and sectioned into slices of 6-μm thickness. Cellular apoptosis was detected by labeling DNA fragments using an ApoMark apoptosis detection kit from Exalpha Biologicals, Inc. (Maynard, MA), according to the manufacturer's instructions. Briefly, the deparaffinized sections were permeabilized with proteinase K and quenched with H_2O_2, and DNA fragments were labeled with biotin-labeled deoxynucleotides by terminal deoxynucleotidyl transferase. After the termination of the reaction, the biotinylated nucleotides were detected using a streptavidin-horseradish peroxidase conjugate that was allowed to react with diaminobenzidine to generate an insoluble colored substrate. Counterstaining was performed with methyl green. The number of TUNEL-positive follicles was counted in at least four sections per ovary, and the data are represented as the average number of TUNEL-positive follicles per ovary section.

Immunohistochemistry

Mouse ovaries were prepared from female mice (age 4–5 weeks) 47 h after injection with PMSG, fixed overnight in 4% paraformaldehyde, embedded in Tissue-Tek compound (Sakura Finetechnical Co., Ltd., Tokyo, Japan), and sectioned into slices of 5-μm thickness. The sections were washed with phosphate-buffered saline, incubated with rabbit anti-LHR primary antibody (1:100) (Santa Cruz Biotechnology, Dallas, TX) overnight at 4 °C, and then with Alexa Fluor 594-conjugated anti-rabbit secondary antibody (Life Technologies, Carlsbad, CA) for 2 h at room temperature. The signals were observed by confocal microscopy (LSM510 META; Carl Zeiss, Oberkochen, Germany), and the intensity was analyzed using LSM510 META software (Carl Zeiss).

Granulosa cell primary culture

Granulosa cells were collected by follicle puncture from the ovaries of 2- to 4-week-old mice primed with or without PMSG. The cells were cultured in DMEM/F12 (Gibco) supplemented with 10% FBS and 100 units of penicillin-streptomycin. For stimulation with hCG, the cells were seeded in 24-well plates, serum starved overnight, and cultured in the presence or absence of 3 ng/ml hCG for up to 17 h. For treatment with U0126, the cells were cultured with 5 μM U0126 for 40 min prior to hCG stimulation for 10 min. The cells were then harvested to prepare the lysates.

Immunoblotting

Granulosa cells or whole ovaries were lysed with a buffer containing 25 mM Tris-HCl, pH 7.5, 150 mM NaCl, 1% Triton X-100, and 5 mM EDTA. Total cell lysates were separated by sodium dodecyl sulfate polyacrylamide gel electrophoresis, and the proteins were transferred to a polyvinyl difluoride membrane and immunoblotted with antibodies against PRIP-1 (1:1000) (17), PRIP-2 (1:1000) (17), LHR (1:1000) (Santa Cruz Biotechnology), FSHR (1:1000) (Boster Immunoleader, Fremont, CA), extracellular signal-regulated kinase (ERK) 1/2 (1:1000) (Cell Signaling Technology, Danvers, MA), phospho-ERK1/2 (Thr202/Tyr204) (1:1000) (Cell Signaling Technology), or β-actin (1:3000) (Sigma-Aldrich). The blots were developed with horseradish peroxidase-coupled secondary antibodies and visualized using an ECL system (Amersham Biosciences, Uppsala, Sweden). The density was quantified using the Image Gauge software (version 3.0; Fujifilm), and the data were shown as relative values.

ELISA

Serum was obtained from 4- to 6-week-old female mice at 24 or 48 h after injection with PMSG, and the E2 and testosterone levels were measured by ELISA (Estradiol EIA Kit, CAY582251, Cayman; Testosterone Assay, KGE010, R&D Systems, Minneapolis, MN). The ovaries were obtained from the same mice and extracts were prepared using a lysis buffer containing 25 mM Tris-HCl, pH 7.5, 150 mM NaCl, 1% Triton X-100, and 5 mM EDTA. The E2 levels were measured using the above method. Serum was also prepared from 6-week-old female mice that were either fed or fasted for 8 h, and the serum insulin level was measured using an insulin ELISA kit (MRD10–1247-01, Mercodia, Uppsala, Sweden). Serum prepared from 6-week-old mice without any treatment was used for the measurement of uncarboxylated OC which was performed using an EIA kit (TaKaRa Bio).

Statistical analysis

The data are presented as the mean ± S.D. of at least three independent experiments. Student's *t*-tests were used for the comparison of groups and p values of < 0.05, 0.01, or 0.001 were considered to indicate statistical significance.

Author contributions—M.M. designed, performed, and analyzed the experiments and the results and wrote the manuscript. M.H. analyzed the data and critically revised the manuscript. Both authors reviewed the results and approved the final version of the manuscript.

Acknowledgments—We thank Professor Ken-ichirou Morohashi and Dr. Takashi Baba (Faculty of Medical Science, Kyushu University) for technical advice, and Kayoko Tsunematsu and Midori Nakagawa for technical assistance. We thank Dr. Kaori Yasuda and Dr. Atsushi Doi (Cell Innovator Inc.) for their skilled technical support for the microarray gene expression analysis and for their helpful discussions. We also thank the Research Support Center, Graduate School of Medical Sciences, Kyushu University.

References

1. Schneider, J. E. (2004) Energy balance and reproduction. *Physiol. Behav.* **81,** 289–317
2. Carel, J. C., and Léger, J. (2008) Clinical practice. Precocious puberty. *N. Engl. J. Med.* **358,** 2366–2377
3. Ehrmann, D. A. (2005) Polycystic ovary syndrome. *N. Engl. J. Med.* **352,** 1223–1236
4. Kanematsu, T., Takeya, H., Watanabe, Y., Ozaki, S., Yoshida, M., Koga, T., Iwanaga, S., and Hirata, M. (1992) Putative inositol 1,4,5-trisphosphate binding proteins in rat brain cytosol. *J. Biol. Chem.* **267,** 6518–6525
5. Yoshida, M., Kanematsu, T., Watanabe, Y., Koga, T., Ozaki, S., Iwanaga, S., and Hirata, M. (1994) D-*myo*-inositol 1,4,5-trisphosphate-binding proteins in rat brain membranes. *J. Biochem.* **115,** 973–980
6. Kanematsu, T., Misumi, Y., Watanabe, Y., Ozaki, S., Koga, T., Iwanaga, S., Ikehara, Y., and Hirata, M. (1996) A new inositol 1,4,5-trisphosphate binding protein similar to phospholipase C-δ1. *Biochem. J.* **313,** 319–325

7. Kanematsu, T., Yoshimura, K., Hidaka, K., Takeuchi, H., Katan, M., and Hirata, M. (2000) Domain organization of p130, PLC-related catalytically inactive protein, and structural basis for the lack of enzyme activity. *Eur. J. Biochem.* **267,** 2731–2737
8. Kanematsu, T., Jang, I.-S., Yamaguchi, T., Nagahama, H., Yoshimura, K., Hidaka, K., Matsuda, M., Takeuchi, H., Misumi, Y., Nakayama, K., Yamamoto, T., Akaike, N., Hirata, M., and Nakayama, K.-I. (2002) Role of the PLC-related, catalytically inactive protein p130 in $GABA_A$ receptor function. *EMBO J.* **21,** 1004–1011
9. Kanematsu, T., Yasunaga, A., Mizoguchi, Y., Kuratani, A., Kittler, J. T., Jovanovic, J. N., Takenaka, K., Nakayama, K. I., Fukami, K., Takenawa, T., Moss, S. J., Nabekura, J., and Hirata, M. (2006) Modulation of $GABA_A$ receptor phosphorylation and membrane trafficking by phospholipase C-related inactive protein/protein phosphatase 1 and 2A signaling complex underlying brain-derived neurotrophic factor-dependent regulation of GABAergic inhibition. *J. Biol. Chem.* **281,** 22180–22189
10. Yoshimura, K., Takeuchi, H., Sato, O., Hidaka, K., Doira, N., Terunuma, M., Harada, K., Ogawa, Y., Ito, Y., Kanematsu, T., and Hirata, M. (2001) Interaction of p130 with, and consequent inhibition of, the catalytic subunit of protein phosphatase 1α. *J. Biol. Chem.* **276,** 17908–17913
11. Fujii, M., Kanematsu, T., Ishibashi, H., Fukami, K., Takenawa, T., Nakayama, K. I., Moss, S. J., Nabekura, J., and Hirata, M. (2010) Phospholipase C-related but catalytically inactive protein is required for insulin-induced cell surface expression of γ-aminobutyric acid type A receptors. *J. Biol. Chem.* **285,** 4837–4846
12. Gao, J., Takeuchi, H., Zhang, Z., Fukuda, M., and Hirata, M. (2012) Phospholipase C-related but catalytically inactive protein (PRIP) modulates synaptosomal-associated protein 25 (SNAP-25) phosphorylation and exocytosis. *J. Biol. Chem.* **287,** 10565–10578
13. Zhang, Z., Takeuchi, H., Gao, J., Wang, D., James, D. J., Martin, T. F., and Hirata, M. (2013) PRIP (phospholipase C-related but catalytically inactive protein) inhibits exocytosis by direct interactions with syntaxin 1 and SNAP-25 through its C2 domain. *J. Biol. Chem.* **288,** 7769–7780
14. Takeuchi, H., Oike, M., Paterson, H. F., Allen, V., Kanematsu, T., Ito, Y., Erneux, C., Katan, M., and Hirata, M. (2000) Inhibition of Ca^{2+} signalling by p130, a phospholipase-C-related catalytically inactive protein: critical role of the p130 pleckstrin homology domain. *Biochem. J.* **349,** 357–368
15. Uji, A., Matsuda, M., Kukita, T., Maeda, K., Kanematsu, T., and Hirata, M. (2002) Molecules interacting with PRIP-2, a novel Ins(1,4,5)P_3 binding protein type 2. Comparison with PRIP-1. *Life Sci.* **72,** 443–453
16. Harada, K., Takeuchi, H., Oike, M., Matsuda, M., Kanematsu, T., Yagisawa, H., Nakayama, K. I., Maeda, K., Erneux, C., and Hirata. (2005) M. Role of PRIP-1, a novel Ins(1,4,5)P3 binding protein, in Ins(1,4,5)P3-mediated Ca^{2+} signaling. *J. Cell Physiol.* **202,** 422–433
17. Terunuma, M., Jang, I. S., Ha, S. H., Kittler, J. T., Kanematsu, T., Jovanovic, J. N., Nakayama, K. I., Akaike, N., Ryu, S. H., Moss, S. J., and Hirata, M. (2004) $GABA_A$ receptor phospho-dependent modulation is regulated by phospholipase C-related inactive protein type 1, a novel protein phosphatase 1 anchoring protein. *J. Neurosci.* **24,** 7074–7084
18. Kanematsu, T., Fujii, M., Mizokami, A., Kittler, J. T., Nabekura, J., Moss, S. J., and Hirata, M. (2007) Phospholipase C-related inactive protein is implicated in the constitutive internalization of $GABA_A$ receptors mediated by clathrin and AP2 adaptor complex. *J. Neurochem.* **101,** 898–905
19. Mizokami, A., Kanematsu, T., Ishibashi, H., Yamaguchi, T., Tanida, I., Takenaka, K., Nakayama, K. I., Fukami, K., Takenawa, T., Kominami, E., Moss, S. J., Yamamoto, T., Nabekura, J., and Hirata, M. (2007) Phospholipase C-related inactive protein is involved in trafficking of γ2 subunit-containing $GABA_A$ receptors to the cell surface. *J. Neurosci.* **27,** 1692–1701
20. Yanagihori, S., Terunuma, M., Koyano, K., Kanematsu, T., Ryu, S. H., and Hirata, M. (2006) Protein phosphatase regulation by PRIP, a PLC-related catalytically inactive protein: implications in the phospho-modulation of the $GABA_A$ receptor. *Adv. Enzyme Regul.* **46,** 203–222
21. Sugiyama, G., Takeuchi, H., Kanematsu, T., Gao, J., Matsuda, M., and Hirata, M. (2013) Phospholipase C-related but catalytically inactive protein, PRIP as a scaffolding protein for phospho-regulation. *Adv. Biol. Regul.* **53,** 331–340
22. Tsutsumi, K., Matsuda, M., Kotani, M., Mizokami, A., Murakami, A., Takahashi, I., Terada, Y., Kanematsu, T., Fukami, K., Takenawa, T., Jimi, E., and Hirata, M. (2011) Involvement of PRIP, phospholipase C-related, but catalytically inactive protein, in bone formation. *J. Biol. Chem.* **286,** 31032–31042
23. Kotani, M., Matsuda, M., Murakami, A., Takahashi, I., Katagiri, T., and Hirata, M. (2015) Involvement of PRIP (phospholipase C-related but catalytically inactive protein) in BMP-induced Smad signaling in osteoblast differentiation. *J. Cell Biochem.* **116,** 2814–2823
24. Murakami, A., Matsuda, M., Harada, Y., and Hirata, M. (2017) Phospholipase C-related, but catalytically inactive protein (PRIP) up-regulates osteoclast differentiation via calcium-calcineurin-NFATc1 signaling. *J. Biol. Chem.* **292,** 7994–8006
25. Matsuda, M., Tsutsumi, K., Kanematsu, T., Fukami, K., Terada, Y., Takenawa, T., Nakayama, K. I., and Hirata, M. (2009) Involvement of phospholipase C-related inactive protein in the mouse reproductive system through the regulation of gonadotropin levels. *Biol. Reprod.* **81,** 681–689
26. March, W. A., Moore, V. M., Willson, K. J., Phillips, D. I., Norman, R. J., and Davies, M. J. (2010) The prevalence of polycystic ovary syndrome in a community sample assessed under contrasting diagnostic criteria. *Hum. Reprod.* **25,** 544–551
27. Feng, Y., Li, X., and Shao, R. (2013) Genetic modeling of ovarian phenotypes in mice for the study of human polycystic ovary syndrome. *Am. J. Transl. Res.* **5,** 15–20
28. Eppig, J. J. (1979) FSH stimulates hyaluronic acid synthesis by oocyte—cumulus cell complexes from mouse preovulatory follicles. *Nature* **281,** 483–484
29. Tsafriri, A. (1995) Ovulation as a tissue remodelling process. Proteolysis and cumulus expansion. *Adv. Exp. Med. Biol.* **377,** 121–140
30. Pepene, C. E. (2013) Serum under-carboxylated osteocalcin levels in women with polycystic ovary syndrome: weight-dependent relationships with endocrine and metabolic traits. *J. Ovarian Res.* **6,** 4
31. Menon, K. M. J., Munshi, U. M., Clouser, C. L., and Nair, A. K. (2004) Regulation of luteinizing hormone/human chorionic gonadotropin receptor expression: a perspective. *Biol. Reprod.* **70,** 861–866
32. Maman, E., Yung, Y., Kedem, A., Yerushalmi, G. M., Konopnicki, S., Cohen, B., Dor, J., and Hourvitz, A. (2012) High expression of luteinizing hormone receptors messenger RNA by human cumulus granulosa cells is in correlation with decreased fertilization. *Fertil. Steril.* **97,** 592–598
33. Orisaka, M., Hattori, K., Fukuda, S., Mizutani, T., Miyamoto, K., Sato, T., Tsang, B. K., Kotsuji, F., and Yoshida, Y. (2013) Dysregulation of ovarian follicular development in female rat: LH decreases FSH sensitivity during preantral–early antral transition. *Endocrinology* **154,** 2870–2880
34. Yung, Y., Aviel-Ronen, S., Maman, E., Rubinstein, N., Avivi, C. R., Orvieto, R., and Hourvitz, A. (2014) Localization of luteinizing hormone receptor protein in the human ovary. *Mol. Hum. Reprod.* **20,** 844–849
35. Foong, S. C., Abbott, D. H., Zschunke, M. A., Lesnick, T. G., Phy, J. L., and Dumesic, D. A. (2006) Follicle luteinization in hyperandrogenic follicles of polycystic ovary syndrome patients undergoing gonadotropin therapy for *in vitro* fertilization. *J. Clin. Endocrinol. Metab.* **91,** 2327–2333
36. Jakimiuk, A. J., Weitsman, S. R., Navab, A., and Magoffin, D. A. (2001) Luteinizing hormone receptor, steroidogenesis acute regulatory protein, and steroidogenic enzyme messenger ribonucleic acids are overexpressed in thecal and granulosa cells from polycystic ovaries. *J. Clin. Endocrinol. Metab.* **86,** 1318–1323
37. Caldwell, J. D., and Jirikowski, G. F. (2014) Sex hormone binding globulin and corticosteroid binding globulin as major effectors of steroid action. *Steroids* **81,** 13–16
38. Doira, N., Kanematsu, T., Matsuda, M., Takeuchi, H., Nakano, H., Ito, Y., Nakayama, K., Nakayama, K. I., and Hirata, M. (2001) Hyperinsulinemia in *PRIP-1* gene deleted mice. *Biomed. Res.* **22,** 157–165
39. Rotterdam ESHRE/ASRM-Sponsored PCOS Consensus Workshop Group. (2004) Revised 2003 consensus on diagnostic criteria and long-term health risks related to polycystic ovary syndrome. *Fertil. Steril.* **81,** 19–25
40. Rotterdam ESHRE/ASRM-Sponsored PCOS Consensus Workshop Group. (2004) Revised 2003 consensus on diagnostic criteria and long-

term health risks related to polycystic ovary syndrome (PCOS). *Hum. Reprod.* **19,** 41–47
41. Franks, S. (1995) Polycystic ovary syndrome. *N. Engl. J. Med.* **333,** 853–861
42. Lan, C. W., Chen, M. J., Tai, K. Y., Yu, D. C., Yang, Y. C., Jan, P. S., Yang, Y. S., Chen, H. F., and Ho, H. N. (2015) Functional microarray analysis of differentially expressed genes in granulosa cells from women with polycystic ovary syndrome related to MAPK/ERK signaling. *Sci. Rep.* **5,** 14994
43. Shelling, A. N. (2010) Premature ovarian failure. *Reproduction* **140,** 633–641
44. Kanamarlapudi, V., Gordon, U. D., and López Bernal, A. (2016) Luteinizing hormone/chorionic gonadotrophin receptor overexpressed in granulosa cells from polycystic ovary syndrome ovaries is functionally active. *Reprod. Biomed. Online* **32,** 635–641
45. Chang, R. J., and Cook-Andersen, H. (2013) Disordered follicle development. *Mol. Cell Endocrinol.* **373,** 51–60
46. Webber, L. J., Stubbs, S. A., Stark, J., Margara, R. A., Trew, G. H., Lavery, S. A., Hardy, K., and Franks, S. (2007) Prolonged survival in culture of preantral follicles from polycystic ovaries. *J. Clin. Endocrinol. Metab.* **92,** 1975–1978
47. Donadeu, F. X., Esteves, C. L., Doyle, L. K., Walker, C. A., Schauer, S. N., and Diaz, C. A. (2011) Phospholipase Cβ3 mediates LH-induced granulosa cell differentiation. *Endocrinology* **152,** 2857–2869
48. Makker, A., Goel, M. M., and Mahdi, A. A. (2014) PI3K/PTEN/Akt and TSC/mTOR signaling pathways, ovarian dysfunction, and infertility: an update. *J. Mol. Endocrinol.* **53,** R103–R118
49. Walters, K. A., Allan, C. M., and Handelsman, D. J. (2012) Rodent models for human polycystic ovary syndrome. *Biol. Reprod.* **86,** 149, 1–12
50. Asano, S., Nemoto, T., Kitayama, T., Harada, K., Zhang, J., Harada, K., Tanida, I., Hirata, M., and Kanematsu, K. (2014) Phospholipase C-related catalytically inactive protein (PRIP) controls KIF5B-mediated insulin secretion. *Biol. Open* **3,** 463–474
51. Davoren, J. B., Kasson, B. G., Li, C. H., and Hsueh, A. J. (1986) Specific insulin-like growth factor (IGF) I- and II-binding sites on rat granulosa cells: relation to IGF action. *Endocrinology* **119,** 2155–2162
52. Eppig, J. J., O'Brien, M. J., Pendola, F. L., and Watanabe, S. (1998) Factors affecting the developmental competence of mouse oocytes grown in vitro: follicle-stimulating hormone and insulin. *Biol. Reprod.* **59,** 1445–1453
53. Mizokami, A., Yasutake, Y., Gao, J., Matsuda, M., Takahashi, I., Takeuchi, H., and Hirata, M. (2013) Osteocalcin induces release of glucagon-like peptide-1 and thereby stimulates insulin secretion in mice. *PLoS One* **8,** e57375
54. Oue, K., Zhang, J., Harada-Hada, K., Asano, S., Yamawaki, Y., Hayashiuchi, M., Furusho, H., Takata, T., Irifune, M., Hirata, M., and Kanematsu, T. (2016) Phospholipase C-related catalytically inactive protein is a new modulator of thermogenesis promoted by β-adrenergic receptors in brown adipocytes. *J. Biol. Chem.* **291,** 4185–4196